

Synthesis, spectra and DNA interactions of certain mononuclear transition metal(II) complexes of macrocyclic tetraaza diacetyl curcumin ligand

Jegathalaprathaban Rajesh^{a,b,*}, Ammavasi Gubendran^{a,c}, Gurusamy Rajagopal^d, Periyakaruppan Athappan^a

^a Department of Inorganic Chemistry, School of Chemistry, Madurai Kamaraj University, Madurai 625 021, India

^b Madurai Institute of Engineering & Technology, Sivagangai 630 611, India

^c Department of Chemistry, Saraswathi Narayanan College, Madurai 625 022, India

^d Department of Chemistry, Government Arts College, Melur, Madurai 625 106, India

ARTICLE INFO

Article history:

Received 20 September 2011

Received in revised form 3 December 2011

Accepted 3 December 2011

Available online 16 December 2011

Keywords:

Benzilidene diacetyl curcumin

Tetraaza metal complexes

Calf thymus DNA

CD spectra

DNA cleavage

ABSTRACT

A series of mononuclear transition metal(II) complexes of type $[M(LL)]^{2+}$ (LL = the template condensate of orthophenylene diamine and benzilidene diacetyl curcumin (ben-diaecur) and M = Cu(II) (**1**) or Co(II) (**2**) or Ni(II) (**3**) or Mn(II) (**4**)), have been isolated and the spectral behaviors are discussed. The ligand and complexes have also been characterized by the analytical and spectral methods like UV–Visible, FT-IR, NMR and EPR. Further, the interaction of the transition metal complexes with Calf thymus (CT) DNA have also been studied by the use of physical methods like UV–Visible, emission and CD spectroscopic techniques. The electrochemical responses of these metal complexes both in presence and absence of DNA have also been demonstrated. All these findings support the hypothesis of DNA interactions of all these metal complexes through the grooves with a higher degree of interaction by complex **1** ($K_b = 1.4 \times 10^5$) possibly through the interposition of the aromatic rings of the ligand compared to complexes, **2–4**. The complex **1** display significant oxidative cleavage of circular plasmid pUC¹⁸ DNA in the presence of H₂O₂ using the singlet oxygen as a reactive species. The spectral and electrochemical response of these complexes designate that the square-planar Cu(II), Ni(II) and Co(II) complexes interact much better than the axially coordinated octahedral Mn(II) complex.

© 2011 Elsevier B.V. All rights reserved.

1. Introduction

Curcumin has been widely used as a yellow pigment to color food, drugs and cosmetics, and it is also interesting from a pharmaceutical point of view because of its potential use as a drug or model substance for treatment of various diseases. The most interesting effects are probably its potential use against cancer, HIV-infections, cystic fibrosis, and as an immuno modulating agent [1–8]. Evaluation of curcumin and structural derivatives in cancer chemoprevention model systems has demonstrated a range of potencies dependent upon particular substituents on the aromatic moiety [9]. Compared to curcumin, diacetylcurcumin (DAC) has been shown to have greater efficiency as an NO scavenger [10]. A manganese diacetylcurcumin complex was significantly more effective as an antioxidant scavenger than the comparable manganese curcumin complex, and displayed neuroprotective effects as well [11]. We expect that new analogs of the curcumin ligand, including DAC, complexed to transition metal complex, might be more effective

than is deacetylated curcumin, as medicinal inorganic therapeutic agents. Thus, we prepared curcumin derivatives by slightly modifying the ligand, then by replacing the hydroxyl substituents on the aromatic rings with acetyl groups in curcumin [10] (Fig. 1). Complexation of metal with a known antioxidant, curcumin, has the potential to improve synergistically the potency of a metal-based hypoglycemic agent [12,13]. Herein, we attempt to further improve on this potential therapeutic efficacy by using curcumin derivatives as tetraaza ligands, complexed to metal ions. In this investigation, we have extended our studies of metal complexation by the β -diketones, curcumin derivatives and four new metal coordination complexes of acetylated curcumin, including copper, cobalt, nickel and manganese-based compounds. A principle objective of this investigation was to evaluate the therapeutic potential of several metal complexes with curcumin and DAC. A corollary objective, relevant to these objectives, was to test the hypothesis that free radical scavenging activity would be impaired, at least partially; in the new acetylated complexes and that this might affect cytotoxicity as well as antioxidant potential, in which the phenolic OH groups, known to be essential for antioxidant activity [14,15], were blocked by acetyl moieties. Curcumin (a natural β -diketone) based Schiff bases can have extensive conjugation, which

* Corresponding author at: Madurai Institute of Engineering & Technology, Sivagangai 630 611, India.

E-mail address: mkuraji@gmail.com (J. Rajesh).

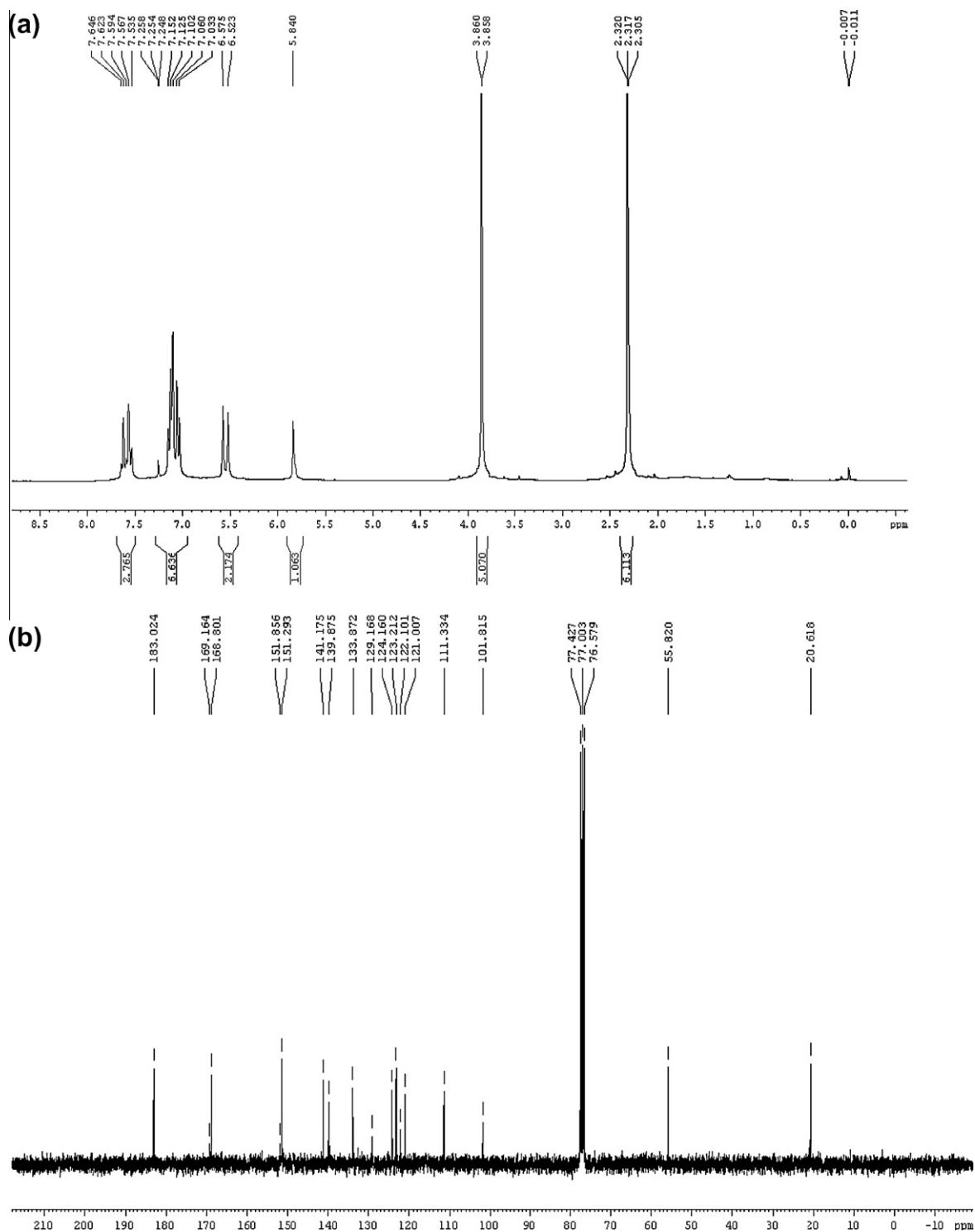


Fig. 1. ¹H NMR (a) and ¹³C NMR (b) spectra of ben-acetyl curcumin recorded in CDCl₃.

could be varied for π -bonding to the central metal ion [16]. With a view to mimicking the functional properties of naturally occurring tetraaza macrocycles and with the aim of adding new metal complexes, an endeavor is made to synthesize a tetraaza 14-membered system with extended conjugation using benzylidene diacetylcurcumin condensed with diamines. Compared to the porphyrin system, this 14-membered tetraaza compound is expected to stabilize the higher oxidation states of the first transition series due to steric reasons. Their Cu(II), Ni(II), Co(II) and Mn(II) com-

plexes have been prepared and characterized through IR, UV-Vis, NMR, EPR spectral methods and by cyclic voltammetry. These tetraaza macrocyclic metal complexes are also expected to interact with DNA as they have phenyl rings. The strong spectrochemical and electrochemical characteristics of these complexes provide sensitive utensils to study their interaction with DNA molecules. The changes in the intensities of the spectral and electrochemical behavior can be used to explore the nature and potency of the interaction between the chromophore and DNA base pairs. Based

on this information, it has been planned to design the tetraaza macrocyclic metal complexes (CuN_4 , CoN_4 , NiN_4 and MnN_4) from benz-acetylcurcumin (non-enolisable β -diketone) and to study their binding efficiency with CT-DNA and the results are discussed. The Cu(II), Co(II), Ni(II) and Mn(II) complexes are respectively designated as complex **1**, **2**, **3** and **4**.

2. Experimental

2.1. Materials and instrumentation

Curcumin (MERCK), *ortho*-phenylenediamine (MERCK), meta-I(II) chlorides (SRL), benzaldehyde (SRL), acetic anhydride (SRL), pyridine (MERCK), Calf thymus DNA (Sigma), Tris-hydrochloride (SRL) and sodium chloride (SRL) were used as received. Double distilled water was used for all the experiments. All reagents and solvents were analytical, spectroscopic grade and they were used without further purification and then used for the preparation of ligands and complexes. The complexes are brown in color and are soluble in DMSO.

Nuclear magnetic resonance spectroscopic measurements were made on a Perkin-Elmer 300 MHz spectrometer. Deuterated organic solvents along with tetramethylsilane (TMS) as the internal standard were used. UV-Vis spectral measurements were made on DMSO solution of the M(II) complexes using JASCO double beam recording spectrophotometer in the range 200–1100 nm. The infrared spectra of all complexes as well as the free ligand were recorded using KBr pellet on a JASCO FT-IR 410 double beam infrared spectrophotometer in the range of 400–4000 cm^{-1} . Electron paramagnetic resonance spectra of the copper and manganese complexes were obtained on a Varian-E-112 EPR spectrometer. The spectra were recorded for solutions of the complexes in DMSO solvent at room temperature (RT) as well as at liquid nitrogen temperature (77 K). 2,2-diphenyl-1-picrylhydrazyl (DPPH) was used as the field marker. Cyclic voltammetric measurements were carried out on a Bio-Analytical System (BAS) model CV-50W electrochemical analyser. The three electrode cell comprising of a reference Ag/AgCl, counter electrode as platinum wire and working glassy carbon (GC) electrodes with surface area of 0.07 cm^2 was used. The GC was polished with 0.3 and 0.005 mm alumina before each experiment and if necessary the electrode was sonicated in distilled water for 10 min. Dissolved oxygen was removed by purging pure nitrogen gas into the solution for about 15 min before each experiment. Scanning the cyclic voltammogram for a blank solution checked the purity of the supporting electrolyte and the solvent.

2.2. Spectroscopic studies on DNA interaction

2.2.1. Electronic absorption spectra

All the experiments involving the interaction of the complexes **1–4** with CT-DNA were carried out in Tris buffer (5 mM, pH 7.2). A solution of CT-DNA in the buffer gave a ratio of UV absorbance at 260 and 280 nm of about 1.8–1.9:1, indicating that the DNA was sufficiently free from protein [17]. The DNA concentration per nucleotide and polynucleotide concentration were determined by absorption spectroscopy using the molar extinction coefficient ($6600 \text{ M}^{-1} \text{ cm}^{-1}$) at 260 nm [18]. The intrinsic binding constant K_b for the interaction of these metal(II) complexes with DNA has been calculated from the absorption spectral titration data. The intrinsic binding constant K_b was determined from [19],

$$[\text{DNA}]/(\varepsilon_a - \varepsilon_f) = [\text{DNA}]/(\varepsilon_b - \varepsilon_f) + 1/K_b(\varepsilon_b - \varepsilon_f) \quad (1)$$

where [DNA] is the concentration of DNA in base pairs, the apparent absorption coefficient ε_a , ε_f and ε_b correspond to $A_{\text{obs}}/[\text{M}]$, the

extinction coefficient of the free compound and the extinction coefficient of the compound when fully bound to DNA, respectively. Plot of $[\text{DNA}]/(\varepsilon_a - \varepsilon_f)$ vs. [DNA] gave a straight line with a slope of $1/(\varepsilon_b - \varepsilon_f)$ and an intercept of $1/K_b(\varepsilon_b - \varepsilon_f)$ and K_b was determined from the ratio of the slope to intercept.

2.2.2. CD spectra

Circular dichroic spectra of DNA in the presence and absence of M(II) complexes **1–4** were recorded on a JASCO J-810 (163–900 nm) spectropolarimeter using a quartz cuvette of 1 mm optical path length at increasing complex/DNA ratio ($r = 0.1$ – 0.6). Each sample solution was scanned in the range of 220–320 nm. Each CD spectrum was collected after averaging over at least four accumulations using a scan speed of 100 nm min^{-1} and a 1 s response time from which the buffer background had been subtracted $[\text{DNA}] = 100 \mu\text{M}$.

2.2.3. Fluorescence spectra

The emission spectra were recorded using JASCO FP-6300 spectrofluorometer. To study the competitive binding of complexes with ethidium bromide, EB was excited at 350 nm in the presence of CT-DNA alone as well as in the presence of the complexes **1–4**. DNA was pretreated with EB in the ratio $[\text{DNA}]/[\text{EB}] = 1$ at 37°C . Fluorescence quenching experiments with metal(II) complexes **1–4** were carried out by consecutive additions of 20 μL aliquots of a $1 \times 10^{-4} \text{ M}$ stock solution of complexes **1–4** on the solution containing the mixture EB/CT-DNA in buffered Tris solution. These EB/CT-DNA solutions were incubated at 30 min and then the quencher was added.

2.2.4. Cyclic voltammetry experiments

Differential pulse voltammetry (DPV) of complexes **1–4** in the presence and absence of DNA were obtained by using Bio-Analytical System (BAS) model CV-50W electrochemical analyser at 27°C using a 50 mM NaCl, 5 mM Tris-HCl buffer (pH 7.2) was used as supporting electrolyte.

2.2.5. DNA cleavage

The cleavage of DNA in presence of activating agents H_2O_2 was monitored using agarose gel electrophoresis. In cleavage reactions supercoiled pUC19 DNA (500 ng) (form I) in 10% DMSO–5 mM Tris-HCl–50 mM NaCl buffer at pH 7.2 was treated with copper(II) complex. The samples were incubated for 1 h duration at 37°C . A loading buffer containing 25% bromophenol blue, 0.25% xylene cyanol and 30% glycerol (3 μL) was added and electrophoresis performed at 60 V for 5 h in Tris-acetate-EDTA (TAE) buffer (40 mM Tris-base–20 mM acetic acid–1 mM EDTA) using 1% agarose gel containing 1.0 l g mL^{-1} ethidium bromide. The cleavage products were irradiated at room temperature with a UV lamp (365 nm, 10 W) and analyzed with a BIORAD Model XI computer controlled electrophoresis power supply.

2.3. Synthesis

Diacetylcurcumin (DAC) was prepared according to the literature method [20]. Curcumin and acetic anhydride were combined in dry pyridine, and recrystallized with EtOAc/hexane (60/40) to give DAC in 93% yield.

2.4. Knoevenagel condensates

The β -diketo system of curcumin largely exists as an enol form due to the stabilization of intra-molecular hydrogen bonding. This type of enolisation also prevents the formation of the required imines. Hence, in order to facilitate the formation of imines, it is necessary to block the enolisation by converting the -methylene

(active methylene) group into a benzylidene derivative. The required benzylidene derivative is readily formed by Knoevenagel condensation between diacetylcurcumin (452 mg, 1 mmol) and benzaldehyde (108 mg, 1 mmol) in the presence of catalytic amount of piperidine in alcoholic medium [16,21]. Yield: 76%, mp: 96–98 °C.

2.5. Preparation of metal complexes

The title complexes were prepared from the modified procedure of previous literature [22,23]. The respective metal salt (1 mmol) and orthophenylenediamine (109 μ L, 1 mmol) were dissolved in methanol in a conical flask and the mixture was refluxed with stirring for about 30 min. To the above solution, benzilidene-acetyl curcumin (574 mg, 1 mmol) in methanol was added and the contents were stirred for an additional period of 24 h. The resulted microcrystalline product thus formed was removed by filtration, washed with methanol and dried *in vacuo*. All the experiments were carried out under dry nitrogen.

3. Results and discussion

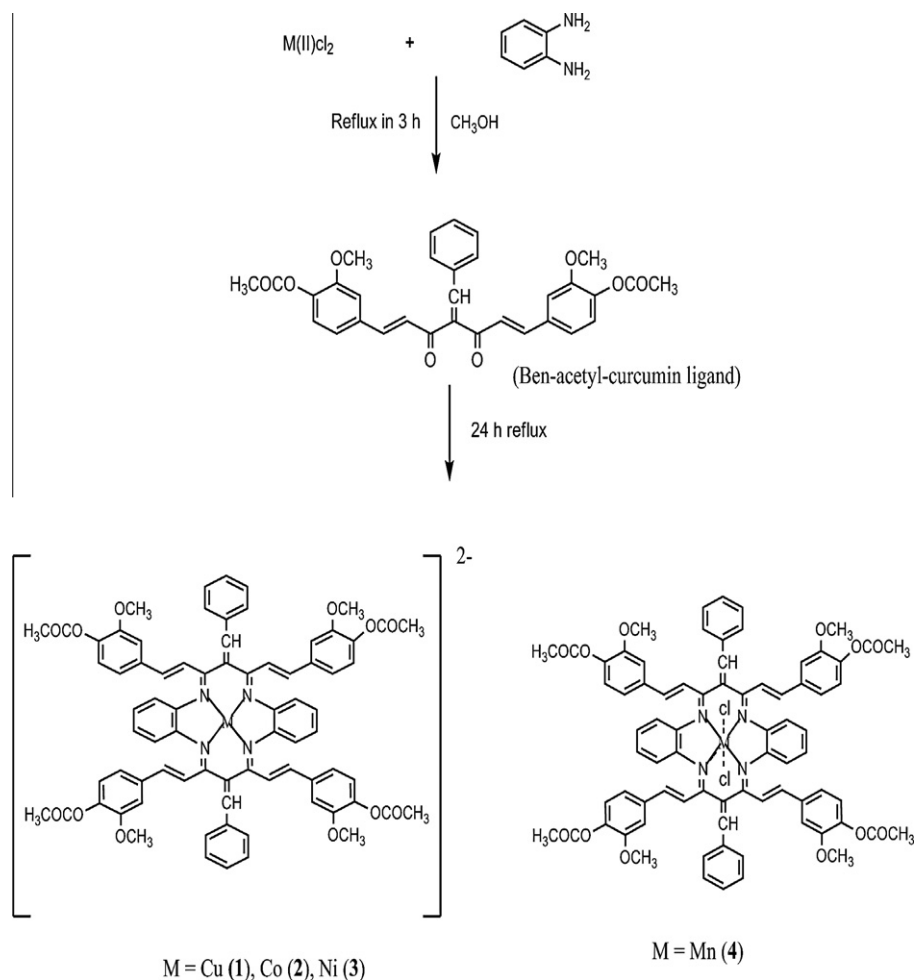
3.1. NMR spectra

Benzilidene diacetylcurcumin (ben-diacetur) (see Scheme 1) dissolved in $CDCl_3$ exhibited all the expected signals. Disappear-

ance of OH proton signal at 9.8 ppm obtained in curcumin together with appearance of new peak at 2.31 ppm corresponding to $COCH_3$ protons clearly confirms acetylation of OH group in curcumin (Fig. 1). The Knoevenagel condensation of benzilidene acetyl curcumin has been further confirmed by the peak observed at 5.8 ppm as a singlet for benzilidene hydrogen. The acetoxy carbon and benzilidene carbon are also observed in the ^{13}C NMR spectra at 20.61 ppm and 168.80 ppm respectively. In the ^{13}C NMR spectra, the number of signals due to aromatic carbons observed in the range 115–152 ppm for benzilidene curcumin is higher than that observed for curcumin which confirms the presence of one more benzene unit in benzilidene curcumin.

3.2. IR spectra

The IR spectra of the starting materials and their metal complexes were recorded and their comparative study has confirmed the formation of macrocyclic complexes with the proposed coordination pattern. The important absorption band of $\nu(C=O)$, at ca. 1630 cm^{-1} in the present benzilidene-diacetylcurcumin (Knoevenagel condensate), has changed upon condensation with amine yielding the tetraaza molecule. In the spectra of tetraaza Schiff base complexes, disappearance of carbonyl band and a new strong sharp band that appears at 1594 cm^{-1} region is attributed to the $\nu(C=N)$ band, confirming the formation of the Schiff base metal(II) complexes [23,24]. The acetate $C=O$ group that shows a strong



Scheme 1. Synthesis of Macrocyclic metal complexes 1–4.

band at $ca. 1767\text{ cm}^{-1}$, does not undergo any shift in complexes as the C=O in acetate group is not involved in bonding. The appearance of a sharp band at 1626 cm^{-1} is assigned to $\nu(\text{C=C})$ of benzylidene [23]. The sharp band in the region $462\text{--}476\text{ cm}^{-1}$ is assigned to $\nu(\text{M-N})$ [25]. The representative spectra of the ligand and the metal complexes are shown in Fig. S1 in the Supporting Information and the values are tabulated in Table S1 in the Supporting Information. The IR spectral data thus confirm the mode of coordination of ligands to the metal.

3.3. UV-Vis spectra

The electronic spectra of complexes **1–4** were recorded in DMSO at room temperature and the values are tabulated in Table S2 in the Supporting Information. The spectrum of free starting ligand exhibits three absorption bands at 260, 318 and 405 nm. These bands are attributed to $\pi\text{--}\pi^*$ and $n\text{--}\pi^*$ transition of the ligand. The electronic spectrum of the Cu(II) complex in DMSO exhibits a d-d band at 669 nm (Fig. S2 in the Supporting Information), which can be assigned to the combination of ${}^2\text{B}_{1g} \rightarrow {}^2\text{E}_g$ and ${}^2\text{B}_{1g} \rightarrow {}^2\text{B}_{2g}$ transitions [26] in a distorted square planar copper(II) environment. The Co(II) complex exhibits a sharp absorption band at 423 nm, and a d-d band at 674 nm which is assignable to the combination of ${}^2\text{B}_{1g} \rightarrow {}^2\text{A}_{1g}$ and ${}^2\text{B}_{1g} \rightarrow {}^2\text{E}_g$ transitions, which are in agreement with square-planar cobalt(II) complexes [27]. The Ni(II) complex is diamagnetic and the band around 428 nm could be assigned to ${}^1\text{A}_{1g} \rightarrow {}^1\text{B}_{1g}$ transition, consistent with other square-planar nickel(II) complexes [28]. The Mn(II) complex exhibits a broad band around 426 nm, which may be assigned to ${}^6\text{A}_{1g} \rightarrow {}^4\text{T}_{2g}$ transition in an octahedral manganese(II) environment [28].

3.4. EPR spectra

EPR spectra of complexes **1** and **4** were recorded in DMSO at liquid nitrogen temperature (77 K), and they show a typical four line pattern for Cu(II) complex and a six line pattern for Mn(II) complex (Fig. 2a and b). From these spectra, g_{\parallel} and g_{\perp} values have been evaluated and were found to be 2.27 and 2.07, respectively, for Cu(II) and Mn(II) complexes. The g_{\parallel} values are greater than the corresponding g_{\perp} values and therefore the complexes should have unpaired electron in its $d_{x^2-y^2}$ molecular orbital. It is reported that g_{\parallel} is a moderately sensitive function for indicating covalency, for a covalent environment g_{\parallel} is normally <2.3 and for ionic environment it should be >2.3 [29,30]. In the present case, the g_{\parallel} values are <2.3 , which indicates covalent environment in the complexes and $G = (g_{\parallel} - 2)/(g_{\perp} - 2) = 3.6$ supporting the square-based geometry around copper(II) in solution. This suggests that these macrocyclic complexes have appreciable covalent character in bonding involving the metal ion and ligand [31]. The observed A_{\parallel} values (Table 1) are in the order of $(186 \times 10^{-4}\text{ cm}^{-1})$ which are consistent with a typical monomeric slightly distorted square-planar structure [32]. Many conjugative CuN_4 macrocyclic systems with smaller hole size place the copper(II) above the plane of the ring [33] thereby reducing the A_{\parallel} values. The observed A_{\parallel} values suggest that such distortion occurs and the Cu(II) complex have a distorted square planar geometry. The observed quotient $g_{\parallel}/A_{\parallel}$ is found to be 146, which indicates moderate distortion from planarity [34]. Magnetic moment values of the Cu(II) complex suggest that it is paramagnetic with μ_{eff} value of 1.89 B.M with one unpaired electron. The EPR spectrum of the manganese(II) complex has been recorded in DMSO solution. The solution sample gives one broad isotropic signal centered at approximately the free electron 'g' value i.e., 2.08 (Table 1) [35]. In DMSO solution, the Mn(II) complex gives EPR signals (Fig. 2b) containing six lines arising due to the hyperfine interaction between the unpaired electron with

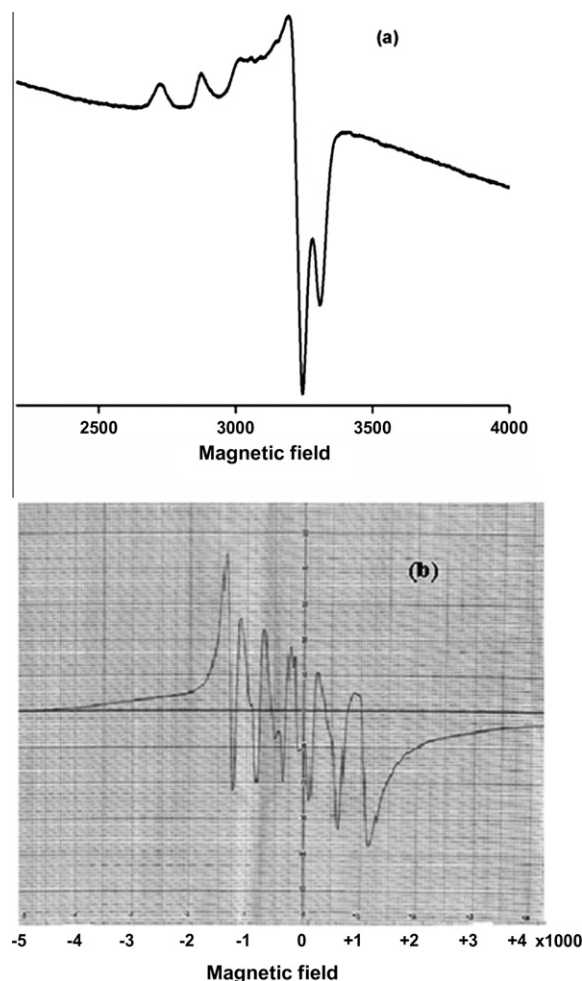


Fig. 2. EPR spectra of complex **1** (a) and complex **4** (b) in DMSO solution at 77 K.

Table 1
EPR spectral data of complexes **1** and **4** in DMSO.

Complexes	g_{\parallel}	g_{\perp}	A_{\parallel} (10^{-4} cm^{-1})	A_{\perp} (10^{-4} cm^{-1})	$g_{\parallel}/A_{\parallel}$	μ_{effect}
1	2.27	2.07	186	50	146	1.89
4	2.10	2.07	178	110	129	6.14

the ${}^{55}\text{Mn}$ nucleus ($I = 5/2$). The nuclear magnetic quantum number M_I , corresponding to these lines are $-5/2, -3/2, -1/2, 0, +1/2, +3/2$ and $+5/2$ from low to the high field. Magnetic moment values of the Mn(II) complex suggest that it is paramagnetic with μ_{eff} value of 6.14 B.M with five unpaired electron.

3.5. Cyclic voltammetry

The cyclic voltammogram of complexes **1–4** were recorded in DMSO at room temperature. The electrochemical data are given in Table S3 in the Supporting Information. The Co(II) and Ni(II) complexes show one well distinct cathodic peak in the range of -771 to -781 mV and the corresponding anodic peak appears in the range of -560 to -592 mV. The measured ΔE_p values clearly indicate that these redox couples are less stable. The Cu(II) and Mn(II) complexes fail to show redox couples and these complexes show only cathodic peaks in the range of -853 to -950 mV. It can be understood from the absence of anodic peak that both the

complexes are irreversible in nature (Fig. S4b in the Supporting Information). The i_{pa}/i_{pc} values for complexes **11** and **12** around 0.5–0.6, clearly confirm one electron redox process and the measured ΔE_p values ($\Delta E_p = 191$ – 211 mV) clearly indicate that these redox couples are quasi-reversible (Fig. S4a in the Supporting Information).

4. DNA binding studies

4.1. Electronic absorption spectra

In buffer solution, the UV–Visible absorption spectra of complexes **1–4** show intense absorption bands in the UV-region, and characteristic CT bands, respectively, at 410, 408, 406 and 371 nm (Table 2). Moreover, the similarity with the UV absorption spectrum of the complex **1** allows inferring that both the cationic complexes **2** and **3** analogously adopt a square planar MN_4 coordination. The UV–Visible absorption spectra of all the metal complexes are significantly perturbed by the addition of increasing amounts of DNA. In detail, the absorption band of complex **1** at 410 nm is red shifted by 6 nm and shows hypochromism of 15%. The absorption band of complex **4** at 406 nm is red shifted by 2 nm and shows hypochromism of 12%. Moreover, the intensity of the absorption band around 264 nm is lowered by the addition of DNA up to $R = 18$, for all the complexes (Fig. 3). All these findings support the hypothesis of DNA interactions of all these metal complexes through the grooves [36] with a higher degree of interaction by complex **1** ($K_b = 1.4 \times 10^5$) possibly through the interposition of the aromatic rings of the ligand compared to complexes, **2–4**. The lowest binding constant of complex **4** ($K_b = 3.5 \times 10^4$) (Table 2) may be due to the presence of two chlorine groups in the axial position and it leads to weak groove binding. The K_b values obtained here are lower than that reported for classical intercalators (for ethidium bromide and [Ru(phen)DPPZ], whose binding constants have been found to be in the order of 10^6 – 10^7 M) [37]. These results suggest an intimate association of the compounds with CT-DNA and it is also likely that compounds bind to the helix *via* groove mode [38].

4.2. Circular dichroism studies

The CD spectrum of CT-DNA recorded in the absence of the metal complexes show a positive band at 275 nm due to base stacking and a negative band at 245 nm due to helicity and is characteristic of DNA in the right-handed *B* form [39]. In the presence of complex **1**, both the positive band at 275 nm and negative band at 245 nm are shifted to higher wavelengths of about 5 nm with increase in intensities (Fig. 4a), which corresponds to induced CD on the hydrophobic interaction of complex **1** with DNA. Such spectral changes are characteristic of *B* to *A* form conformational change

Table 2

Ligand-based absorption spectral properties of metal(II) complexes, **1–4** bound^a to CT-DNA.

Complexes	λ_{\max} (nm)		Hypochromism <i>H</i> (%)	Red shift $\Delta\lambda$ (nm)	Binding constant K_b (M^{-1})
	Free	Bound			
1	410	416	15	6	1.4×10^5
2	408	413	12	5	5.2×10^4
3	371	373	14	2	5.3×10^4
4	406	408	12	2	3.5×10^4

^a Measurements made at different *R* values, where $R = [DNA]/[complex]$, concentrations of solutions of metal(II) complexes in pH 7.2 in 10% DMSO–buffer solutions = 1.0×10^{-5} M (**1**), 1.0×10^{-5} M (**2**), 1.0×10^{-5} M (**3**), 1.0×10^{-5} M (**4**).

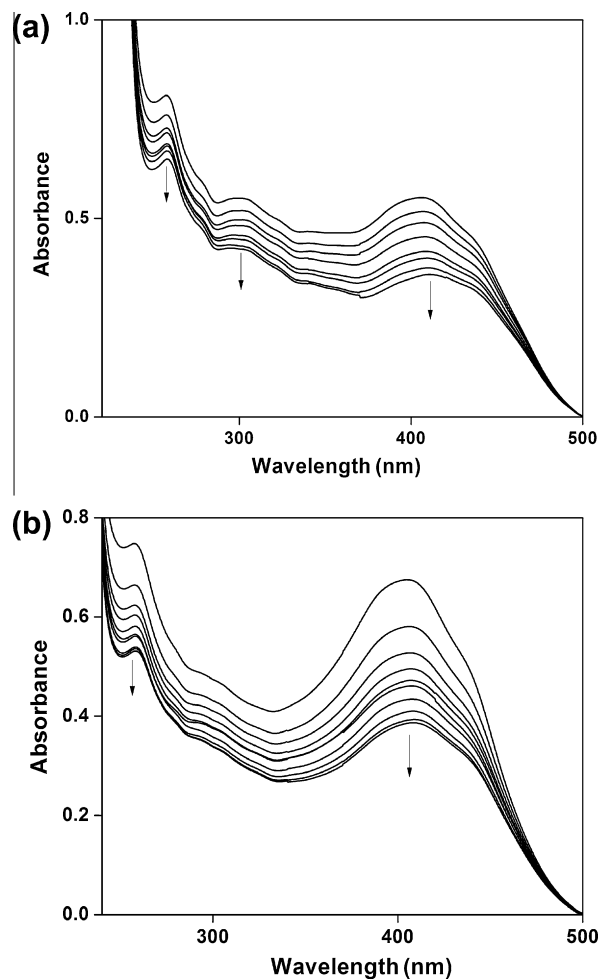


Fig. 3. Absorption spectra of complex **1** (1.0×10^{-5} M) (a), complex **4** (1.0×10^{-5} M) (b) in Tris–HCl buffer pH 7.2 in the absence ($R = 0$) and presence ($R = 2, 4, 6, \dots, 8$) of increasing amounts of DNA. $R = [DNA]/[complex]$. Arrow mark indicates the absorbance change upon increasing DNA concentration.

[40]. This shift in the positive and negative ellipticity band from 275 to 280 nm and 245 to 250 nm respectively supports this type of transformation and it is proposed that in order to accommodate complex bulkier in nature the conversion of *B* to *A* form of DNA which has a major groove to accommodate such molecules is effected on increasing the concentration of complex **1**, the positive band at 280 nm and negative band at 250 nm are shifted to higher wavelength region (Table 3). This effect is attributed to intra-stand linking of adjacent guanines so that the DNA conformation is modified and restacking of the adjacent bases occurs.

In the CD spectra, the addition of complex **2** ($r = 0.1$ – 0.6) to the solution of DNA induced a decrease in intensity in both positive and negative bands (Fig. 4b), suggesting that the stacking mode and the orientation of base pairs in DNA were disturbed. The outcome result shows that the cobalt(II) complex is clearly compatible with a drug-inducible transition to an *A* form. This suggests that the DNA binding of the complexes induces certain conformational changes, such as the conversion from a more *B*-like to a more *A*-like structure with in the DNA molecule [41,42]. Furthermore, with increasing concentration of complex the peaks at 275 and 245 nm are shifted to 1–2 nm without any change in the zero-cross over at 258 nm. Similar observations are also observed for complexes **3** and **4**. These observations also indicate that the DNA interacts with complexes **2–4** through the minor grooves. Moreover the presence of two bulky benz-diacetyl curcumin is responsible for

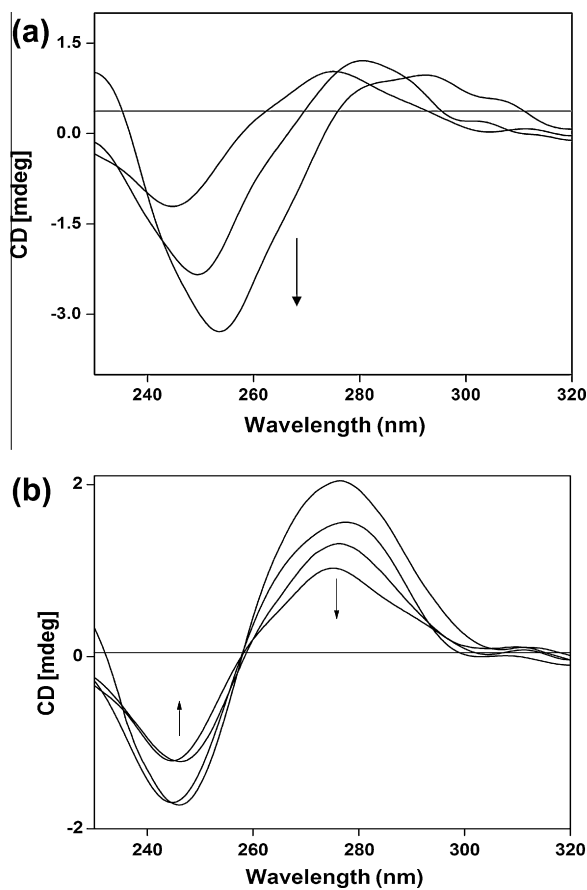


Fig. 4. Circular dichroism spectra of CT DNA in the absence ($r = 0$) and in presence of complexes **1** (a) and **2** (b) ($r = 0-0.3$); [CT DNA] = 100 μM . Cell path length = 1 mm. Arrow mark indicates the molar ellipticity change upon increasing complexes concentration.

Table 3
CD parameters for the interaction of CT-DNA with metal(II) complexes, **1–4** bound^a to CT-DNA

Complexes	r	Positive band		Negative band	
		λ_{max} (nm)	CD (mdeg)	λ_{max} (nm)	CD (mdeg)
DNA	–	275	1.0278	245	–1.2097
1	0.10	280	1.2239	250	–2.2989
	0.20	294	1.0070	254	–3.3651
	0.30	298	0.6263	261	–1.5419
	2	0.10	278	1.0278	245
	0.20	276	1.1500	245	–1.1880
	0.30	276	1.3945	246	–1.2097
3	0.10	276	3.9621	246	–4.8961
	0.20	276	1.4047	245	–1.6746
	0.30	277	1.1154	246	–1.3352
4	0.10	277	2.0317	246	–2.3284
	0.20	275	0.9553	244	–1.3575
	0.30	276	0.9161	244	–1.1209

^a Measurements made at different r values, where $r = [\text{complex}]/[\text{DNA}]$, [DNA] = 100 μM . Cell path length = 1 mm

the lack of intercalation with DNA. The interaction of complexes with DNA in their grooves may therefore be attributed to be primarily via the diamine moiety, rather than the benz-diacetyl curcumin. These changes are indicative of a nonintercalative mode of binding of these complexes and offer support to their groove binding nature [43].

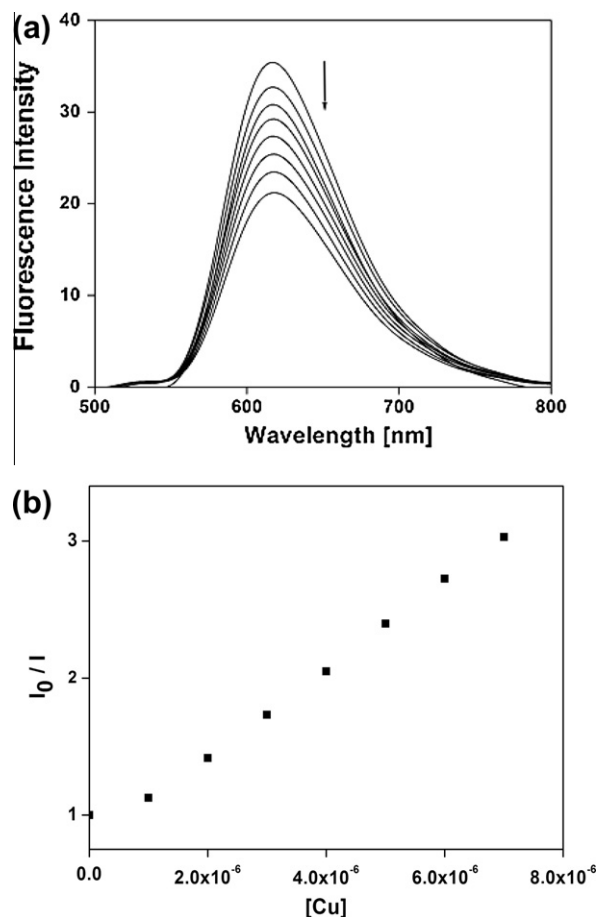


Fig. 5. (a) Emission spectra of EB-DNA in the absence ($r = 0$) and presence ($r = 0, 1, 2, 3, \dots, 7$) of various concentrations of complexes **1**. Arrows indicate the direction of change upon increasing concentration of complex **1**. $r = [\text{complex}]/[\text{EB-DNA}]$; $\lambda_{\text{ex}} = 350$ nm; $\lambda_{\text{em}} = 618$ nm. (b) The fluorescence quenching curve of EB bound to DNA by complex **1** vs. I_0/I . [EB] = 1 μM , [DNA] = 100 μM .

4.3. Emission studies

The binding of complexes **1–4** to the CT-DNA has been studied by fluorescence spectral method. For complexes **1–4**, no emission was observed either in Tris buffer or in the presence of DNA; it is also found that photoluminescence was not shown in any of the organic solvents examined. Steady-state competitive binding experiments using complexes **1–4** as quencher may afford further information to study the binding of the complex to DNA. As we know, ethidium bromide (EB) emits intense fluorescence in the presence of DNA. It was previously reported that the enhanced fluorescence can be quenched, at least partially by the addition of a second molecule [44–46]. The extent of quenching of fluorescence intensity of EB bound to DNA is used to determine the extent of binding between the second molecule and DNA. The emission spectra of EB bound to DNA in the absence and the presence of complex **1** are shown in Fig. 5a. The quenching constant K_{SV} was determined from the classical Stern–Volmer [47]:

$$I_0/I = 1 + K_{SV} [Q] \quad (2)$$

where I_0 and I are the fluorescence intensities in the absence and presence of complexes, respectively. K_{SV} is the linear Stern–Volmer quenching constant, $[Q]$ is the concentration of the M(II) (quencher) complexes [47]. The fluorescence quenching curve of DNA-bound EB by complex **1** (Fig. 5b) illustrates that the quenching of EB bound to DNA by complex **1** is in good agreement with the linear curve of

Table 4
Emission spectral properties of metal(II) complexes, **1–4** bound^a to CT-DNA.

Complexes	λ_{emis} (nm)		Hypochromism H (%)	Red shift $\Delta\lambda$ (nm)	Quenching constant K_{SV} (M^{-1})	R^2
	Free	Bound				
1	618	622	66.0	3	1.9×10^5	0.9910
2	618	622	52.3	3	6.9×10^4	0.9971
3	618	619	40.0	1	5.3×10^4	0.9903
4	618	619	38.4	1	4.7×10^4	0.9927

^a Measurements made at different r values, where $r = [\text{complex}]/[\text{EB-DNA}]$, $[\text{DNA}] = 100 \mu\text{M}$.

Stern–Volmer equation. In the linear fit plot of I_0/I vs. $[\text{complex}]/[\text{DNA}]$, K_{SV} is given by the ratio of the slope to intercept and the quenching constant value is $4.7\text{--}19 \times 10^4$ (Table 4). The decrease in the fluorescence intensity thus proves the partial replacement of EB bound to DNA by complexes **1–4**. From the Fig. 5b it is obvious that, we can also know 50% of EB molecules were replaced from DNA-bound EB. As the complex molecule is bulkier in nature, it is not expected to intercalate in between the base pairs and to replace the EB molecule, but due to the conversion of DNA from form *B* to *A* on interaction with the complexes, the release of EB molecules are inevitable and hence the decrease in intensity.

4.4. Electrochemical studies

Electrochemical investigation of drug–DNA interactions can provide a useful complement to other methods and yield information about the mechanism of interaction and the conformation of adduct [48]. The electrochemical behavior of all these complexes and their interaction with DNA were carried out by DPV method. For complexes **1–4**, the voltammetric behavior was studied by DPV, which is shown in (Fig. 6). On increasing the concentrations of DNA, the peak currents decreased, while both the E_{pc} and $E^{0'}$ shifted to less negative potentials (20–60 mV) (Table 5). The shift in $E^{0'}$ and decrease in peak current implies the formation of a new association complex species. Based on the shift in formal potentials of the DPV, the interaction mode of the complexes with DNA can be inferred [49]. Among the three kinds of binding modes for small molecules to DNA, Bard has reported [50] that if $E^{0'}$ shifted to more negative value when small molecules interacted with DNA, the interaction mode is electrostatic or groove binding. On the contrary, if $E^{0'}$ shifted to more positive value, the interaction mode is intercalative binding. Therefore, in the light of Bard's

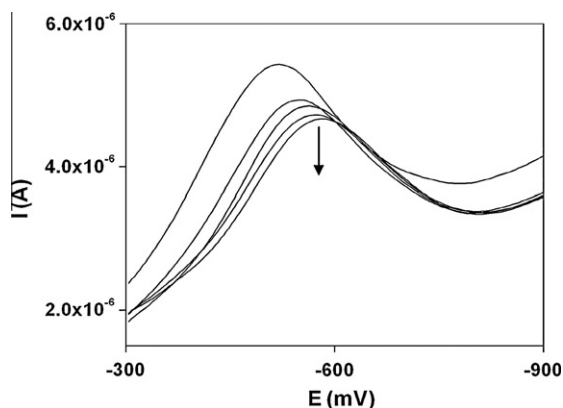


Fig. 6. Differential pulse voltammograms of complex **1** in Tris–HCl buffer pH = 7.2. $R = [\text{DNA}]/[\text{complex}]$; $[\text{complex}] = 0.5 \text{ mM } \mu\text{M}$; $[R = 0, 4, 8, \dots, 16]$. Arrow mark indicates the current change upon increasing DNA concentration.

Table 5

Voltammetric behavior^a of various metal(II) complexes **1–4** in the absence and presence of CT-DNA.

Complexes	R	E_{pc} (mV)	$E_{1/2}$ (mV)	$\Delta E_{1/2}$ (V)	K_{1+}/K_{2+}
1	0	–543	–518	–0.031	1.001
	2	–545	–520	–0.020	
	4	–550	–525	–0.007	
	6	–563	–538	–0.002	
	10	–574	–549		
2	0	–628	–603	–0.056	1.010
	2	–652	–627	–0.045	
	4	–670	–645	–0.042	
	6	–673	–648	–0.024	
	10	–684	–659		
3	0	–623	–598		1.002
	2	–649	–624	–0.049	
	4	–653	–628	–0.042	
	6	–665	–640	–0.030	
	10	–672	–647		
4	0	–609	–584	–0.026	1.001
	2	–633	–608	–0.024	
	4	–640	–615	–0.031	
	6	–650	–625	–0.041	
	10	–661	–636	–0.052	

Differential pulse voltammetry (DPV) at the scan rate of 100 mV s^{-1} , pulse height 50 mV , measured vs. Ag/AgCl with supporting electrolyte $5 \text{ mM Tris-HCl } 50 \text{ mM}$ (pH = 7.2); complex concentration $50 \mu\text{M}$.

^a $E_{1/2}$ values were determined from the DPV of cathodic peak potential E_{pc} , using the relation $E_{1/2} = E_p + \Delta E/2$, where $E_{1/2}$ is the equivalent of the average of E_{pc} and E_{pa} in CV experiments.

report, all complexes interact with DNA by groove binding and/or electrostatic due to negative shift of $E^{0'}$ in all these cases. The shift in the value of the formal potential ($E^{0'}$) can be used to estimate the ratio of equilibrium binding constants k_+/k_{2+} according to the model of interaction described by Carter et al. [50]. From this model one can obtain that

$$E_b^{0'} - E_f^{0'} = 0.059 \log(k_+/k_{2+}) \quad (3)$$

where $E_b^{0'}$ and $E_f^{0'}$ are the formal potentials of the $M(\text{II})/M(\text{I})$ couple in the free and bound forms respectively and k_+ and k_{2+} the corresponding binding constants for the binding of the +1 and +2 species to DNA, respectively. For the complexes **1–4** the $K_{(1)}/K_{(11)}$ values were calculated to be 1.0 suggesting that both the oxidized and reduced forms interact with DNA almost to the same extent. The present study suggested that the complexes **1–4** may interact with DNA in the mode of groove binding [42,51], which is consistent with the above spectral results. Additionally, upon the addition of CT-DNA, the voltammetric currents of the complexes **1–4** decreased. This decrease can be explained in terms of the slow diffusion of the complexes bound to the large DNA molecule. In the present complexes, the aromatic moiety binds with DNA weakly through intercalative mode and predominantly via groove mode through electrostatic interaction with the negatively charged deoxyribose-phosphate backbone [52–55]. The slight shift in formal potential may be due to very weak binding through the grooves or axial interaction of the DNA species to Mn(II) ions.

4.5. DNA cleavage study

The complex **1**, which shows stronger DNA binding affinity and has the ability to change the *B*-form conformation, has been investigated by gel electrophoresis. There is a substantial and continuing interest in DNA endonucleolytic cleavage reactions that are activated by metal ions [56,57]. The interaction of Cu(II) complex with super coiled pUC18 DNA in 10% DMSO–5 mM Tris–HCl buffer pH 7.2 was studied by agarose gel electrophoresis. The DNA ($30 \mu\text{M}$

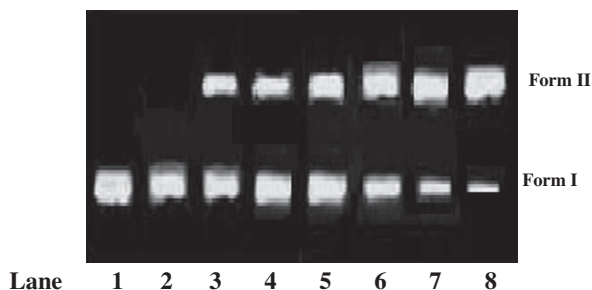


Fig. 7. Agarose gel electrophoresis diagram showing the cleavage of SC pUC18 DNA (500 ng) by complex **1** in Tris-HCl buffer 7.1. Lane 1: DNA control, Lane 2: Lane 1 +30 μM H_2O_2 , Lanes 3–8 in the different concentrations of complex **1** with H_2O_2 (30 μM): (3) 20 μM ; (4) 40 μM ; (5) 60 μM ; (6) 80 μM ; (7) 100 μM and (8) 120 μM .

base pairs) was incubated with various concentrations of Cu(II) complex for 1 h and then subjected to gel electrophoresis. When circular plasmid DNA is subjected to electrophoresis, relatively fast migration will be observed for the intact super coil form (Form I). Fig. 7 shows gel electrophoresis separation of pUC18 DNA after incubation with Cu(II) complex with an oxidizing agent, H_2O_2 . No DNA cleavage was observed for controls in which complex was absent (lane 1), or incubation of the plasmid with the H_2O_2 (lane 2). With increasing concentration of the Cu(II) complexes (lanes 3–8), the intensity of form I of pUC18 DNA diminishes gradually with concomitant increase in the form II intensity. At the concentration of 120 μM , complex **1** almost promotes the complete conversion of DNA from form I to form II.

5. Conclusions

In summary, $[\text{M}(\text{LL})]^{2+}$ complexes, Cu(II), Co(II), Ni(II) and Mn(II), have been synthesized and characterized by UV-Vis, IR, EPR, ESI mass spectra and cyclic voltammetric studies. The interaction between these metal(II) complexes and CT-DNA has been investigated using UV-Vis, fluorescence, CD, cyclic voltammetry and gel electrophoresis. The results obtained collectively show that these macrocyclic metal(II) complexes strongly interact with CT-DNA, by a groove binding mode. The interaction occurrence is supported by the following findings:

- (i) The high value of K_b [$(0.35\text{--}1.4) \times 10^5 \text{ M}^{-1}$], considerable red shift, and the hypochromism of the UV absorption band around 410 nm.
- (ii) The changes in both the band position and intensities of CT-DNA in CD spectra.
- (iii) The decrease in the fluorescence intensity of EB-DNA solution during addition of increasing amount of macrocyclic complexes.
- (iv) Positive shift of both the E_{pc} and $E^{0'}$ (20–60 mV) along with the peak currents decrease in cyclic voltammetry.
- (v) With increasing concentration of the Cu(II) complexes, the intensity of form I of pUC18 DNA diminishes gradually with concomitant increase in the form II intensity.

Acknowledgment

We thank the *University with Potential for Excellence Programme for Madurai Kamaraj University* from UGC, New Delhi, for the financial assistance in the form of a project.

Appendix A. Supplementary material

Supplementary data associated with this article can be found, in the online version, at doi:10.1016/j.molstruc.2011.12.002.

References

- [1] B.B. Aggarwal, A. Kumar, A.C. Bharti, *Anticancer Res.* 23 (2003) 363–398.
- [2] H.P. Ammon, M.A. Wahl, *Planta Med.* 57 (1991) 1–7.
- [3] J.L. Arbisser, N. Klauber, R. Rohan, R.V. Leeuwen, M.T. Huang, C. Fisher, E. Flynn, H.R. Byers, *Mol. Med.* 4 (1998) 376–383.
- [4] M.A. Azuine, S.V. Bhide, *Nutr. Cancer* 17 (1992) 77–83.
- [5] J.H. Kim, J.S. Shim, S.K. Lee, K.W. Kim, S.Y. Rha, H.C. Chung, H.J. Kwon, *Jpn. J. Cancer Res.* 93 (2002) 1378–1385.
- [6] K.H. Thompson, J.H. McNeill, *C. Orvig, Chem. Rev.* 99 (1999) 2561–2572.
- [7] J.H. McNeill, V.G. Yuen, H.R. Hoveyda, C. Orvig, *J. Med. Chem.* 35 (1992) 1489–1491.
- [8] K.H. Thompson et al., *J. Biol. Inorg. Chem.* 8 (2003) 66–74.
- [9] S. Gafner, S.K. Lee, M. Cuendet, S. Barthelemy, L. Vergnes, S. Labidalle, R.G. Mehta, C.W. Boone, J.M. Pezzuto, *Phytochemistry* 65 (2004) 2849–2859.
- [10] Y. Sumanont, Y. Murakami, M. Tohda, O. Vajragupta, K. Matsumoto, H. Watanabe, *Biol. Pharm. Bull.* 27 (2004) 170–173.
- [11] O. Vajragupta, P. Boonchoong, H. Watanabe, M. Tohda, N. Kammassud, Y. Sumanont, *Free Rad. Biol. Med.* 35 (2003) 1632–1644.
- [12] L.C.Y. Woo, V.G. Yuen, K.H. Thompson, J.H. McNeill, C. Orvig, *J. Inorg. Biochem.* 76 (1999) 251–257.
- [13] T. Storr, D. Mitchell, P. Buglyo, K.H. Thompson, V.G. Yuen, J.H. McNeill, C. Orvig, *Bioconjugate Chem.* 14 (2003) 212–221.
- [14] P. Venkatesan, M.N.A. Rao, J. Pharm. Pharmacol. 52 (2000) 1123–1128.
- [15] S.V. Jovanovic, C.W. Boone, S. Steenken, R.B. Kaskey, *J. Am. Chem. Soc.* 123 (2001) 3064–3068.
- [16] J. Annaraj, S. Srinivasan, K.M. Ponvel, P.R. Athappan, *J. Inorg. Biochem.* 99 (2005) 669–676.
- [17] S. Satyanarayana, J.C. Dabrowiak, J.B. Chaires, *Biochemical* 32 (1993) 2573–2584.
- [18] J.K. Barton, J.M. Goldberg, C.V. Kumar, N.J. Turro, *J. Am. Chem. Soc.* 108 (1986) 2081–2088.
- [19] A.M. Pyle, J.P. Rehmman, R. Meshoyrer, C.V. Kumar, N.J. Turro, J.K. Barton, *J. Am. Chem. Soc.* 111 (1989) 3053–3063.
- [20] R.A. Sharma, S.A. Euden, S.L. Platton, D.N. Cooke, A. Shafayat, H.R. Hewitt, T.H. Marczylo, B. Morgan, D. Hemingway, S.M. Plummer, M. Pirmohamed, A.J. Gescher, W.P. Steward, *Clin. Cancer Res.* 10 (2004) 2854–2867.
- [21] J.P. Annaraj, K.M. Ponvel, P.R. Athappan, *Trans. Met. Chem.* 29 (2004) 722–727.
- [22] M. Shakir, O.S.M. Nasman, A.K. Mohamed, S.P. Varkey, *Polyhedron* 15 (1996) 1283–1287.
- [23] S. Srinivasan, G. Rajagopal, P.R. Athappan, *Trans. Met. Chem.* 26 (2001) 588–593.
- [24] P.J. Lukes, A.C. McGregor, T. Clifford, J.A. Crayston, *Inorg. Chem.* 31 (1992) 4697–4699.
- [25] K. Sakata, M. Hashimoto, T. Hamada, S. Matsuno, *Polyhedron* 15 (1996) 967–972.
- [26] S. Tabassum, A. Bashar, F. Arjmand, K.S. Siddiqu, *Synth. React. Inorg. Met.-Org. Chem.* 27 (1997) 487–503.
- [27] P. Chaudhuri, K. Oder, *J. Chem. Soc. Dalton Trans.* (1990) 1597–1605.
- [28] C. Natarajan, P. Tharmaraj, R. Murugesan, *J. Coord. Chem.* 26 (1992) 205–213.
- [29] M.S. Surendra Babu, K. Hussain Reddy, P.G. Krishna, *Polyhedron* 26 (2007) 572–580.
- [30] P. Bindu, M.R. Prathapachandra Kurup, T.R. Satyakeerty, *Polyhedron* 18 (1999) 321–331.
- [31] R.S. Drago, *Phys. Methods Inorg. Chem.* 335 (1991).
- [32] L.M.D. Chia, S. Radojevic, I.J. Scowen, M. McPartlin, M.A. Halcrow, *J. Chem. Soc. Dalton Trans.* (2000) 133–140.
- [33] P. Tamil Selvi, M. Murali, M. Palaniandavar, M. Köckerling, G. Henkel, *Inorg. Chim. Acta* 340 (2002) 139–146.
- [34] G. Rajagopal, N. Prasanna, P.R. Athappan, *Trans. Met. Chem.* 24 (1999) 251–257.
- [35] S. Chandra, S.D. Sharma, *Trans. Met. Chem.* 27 (2002) 732–735.
- [36] J. Liu, H. Zhang, C. Chen, H. Deng, T. Lu, L. Ji, *J. Chem. Soc. Dalton Trans.* (2003) 114–119.
- [37] M. Cory, D.D. McKee, J. Kagan, D.W. Henry, J.A. Miller, *J. Am. Chem. Soc.* 107 (1985) 2528–2536.
- [38] Z.H. Xu, F.J. Chen, P.X. Xi, X.H. Liu, Z.Z. Zeng, *J. Photochem. Photobiol. A* 196 (2008) 77–83.
- [39] P. Lincoln, E. Tuite, B. Norden, *J. Am. Chem. Soc.* 119 (1997) 1454–1455.
- [40] P.U. Maheswari, M. Palaniandavar, *J. Inorg. Biochem.* 98 (2004) 219–230.
- [41] A.K. Patra, M. Nethaji, A.R. Chakravarthy, *J. Inorg. Biochem.* 101 (2007) 233–244.
- [42] P.-x. Xi et al., *J. Inorg. Biochem.* 103 (2009) 210–218.
- [43] Z. Zhang, X.H. Qian, *Int. J. Biol. Macromol.* 38 (2006) 59–64.
- [44] A. Wolf, G.H. Shimer, T. Meehan, *Biochemistry* 26 (1987) 6392–6396.
- [45] B. Peng, H. Chao, B. Sun, H. Li, F. Gao, L.N. Ji, *J. Inorg. Biochem.* 101 (2007) 404–411.
- [46] J.Z. Wu, L. Yuan, J.F. Wu, *J. Inorg. Biochem.* 99 (2005) 2211–2216.

- [47] P.X. Xi, Z.H. Xu, X.H. Liu, F.J. Chen, Z.Z. Zeng, *Chem. Pharm. Bull.* 56 (2008) 541–546.
- [48] M.S. Ibrahim, *Anal. Chim. Acta* 443 (2001) 63–72.
- [49] X. Lu, K. Zhu, M. Zhang, H. Liu, J. Kang, *J. Biochem. Biophys. Methods* 52 (2002) 189–200.
- [50] M.T. Carter, M. Rodriguez, A.J. Bard, *J. Am. Chem. Soc.* 111 (1989) 8901–8911.
- [51] T.S. Pitchumony, P. Mallayan, *Inorg. Chim. Acta* 337 (2002) 420–428.
- [52] S.S. Zhang, S.Y. Niu, B. Qu, G.F. Jie, H. Xu, C.F. Ding, *J. Inorg. Biochem.* 99 (2005) 2340–2347.
- [53] S. Mahadevan, M. Palaniandavar, *Inorg. Chim. Acta* 254 (1997) 291–302.
- [54] Z. Shu-Sheng et al., *Chin. J. Chem.* 23 (2005) 543–547.
- [55] Z. Ji, J. Li, B. Zhu, G. Yuan, S. Cai, *Electrochem. Commun.* 9 (2007) 1667–1671.
- [56] S. Sitlani, E.C. Long, A.M. Pyle, J.K. Barton, *J. Am. Chem. Soc.* 114 (1992) 2303–2312.
- [57] X.W. Liu, J. Li, H. Li, K.C. Zheng, H. Chao, L.N. Ji, *J. Inorg. Biochem.* 100 (2006) 385–395.